

UC Irvine

UC Irvine Previously Published Works

Title

Dose simulations of an early 20th century kilovoltage pneumonia radiotherapy technique performed with a modern fluoroscope

Permalink

<https://escholarship.org/uc/item/4dd8h16b>

Journal

Medical Dosimetry, 46(1)

ISSN

0958-3947

Authors

Roa, Dante
Moyses, Harry
Leon, Stephanie
[et al.](#)

Publication Date

2021

DOI

10.1016/j.meddos.2020.08.002

Peer reviewed



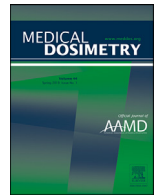
Since January 2020 Elsevier has created a COVID-19 resource centre with free information in English and Mandarin on the novel coronavirus COVID-19. The COVID-19 resource centre is hosted on Elsevier Connect, the company's public news and information website.

Elsevier hereby grants permission to make all its COVID-19-related research that is available on the COVID-19 resource centre - including this research content - immediately available in PubMed Central and other publicly funded repositories, such as the WHO COVID database with rights for unrestricted research re-use and analyses in any form or by any means with acknowledgement of the original source. These permissions are granted for free by Elsevier for as long as the COVID-19 resource centre remains active.



ELSEVIER

Medical Dosimetry

journal homepage: www.meddos.org

Dose simulations of an early 20th century kilovoltage pneumonia radiotherapy technique performed with a modern fluoroscope

Dante Roa, Ph.D.^{*1}, Harry Moyses, M.D.^{*}, Stephanie Leon, Ph.D.[†], Barbara Hamrick, J.D.[‡], Gustavo R. Sarria, M.D.[§], Benjamin Li, M.D.^{||}, Toshiki Tajima, Ph.D.[¶], Ales Necas, Ph.D.[#], Carmen Guzman, Ph.D.^{**}, Oliver Paucar, B.S.^{††}, Alberto Gonzales, B.S.^{‡‡}, Roger Challco, M.S.^{‡‡}, Modesto Montoya, Ph.D.^{‡‡}, Zintia Arqque, B.S.^{‡‡}, Andres Gonzales, M.S.^{§§}, Jimmy Hernandez, M.S.^{|||}, Johnny Drake, B.S.^{¶¶}, Ron Villane, Ph.D.^{¶¶}, Jon Lea, Ph.D.^{##}

^{*} Department of Radiation Oncology, University of California, Irvine Health, Orange, CA 92868, USA

[†] Department of Radiology, University of Florida, Gainesville, FL 32610, USA

[‡] Environmental Health and Safety, University of California, Irvine Health, Orange, CA 92868, USA

[§] Department of Radiation Oncology, University Hospital Bonn, University of Bonn, Bonn, Germany

^{||} Department of Radiation Oncology, University of California, San Francisco, CA 94115, USA

[¶] Department of Physics and Astronomy, University of California, Irvine, CA 92697, USA

[#] TAE Technologies, Foothill Ranch, CA 92610, USA

^{**} Facultad de Ciencias Naturales y Matematica, Universidad Nacional Federico Villarreal, Lima, Peru

^{††} Facultad de Ingenieria Electrica y Electronica, Universidad Nacional de Ingenieria, Lima, Peru

^{‡‡} Facultad de Ciencias, Universidad Nacional de Ingenieria, Lima, Peru

^{§§} Clinica Aliada contra el Cancer, Lima, Peru

^{|||} HRS Oncology International, Las Vegas, NV 89119, USA

^{¶¶} Ziehm Imaging, Orlando, FL 32822, USA

^{##} GE Healthcare, Salt Lake City, UT 84116, USA

ARTICLE INFO

Article history:

Received 15 July 2020

Revised 30 July 2020

Accepted 20 August 2020

Keywords:

Radiotherapy
Pneumonia
Kilovoltage x-rays
Low dose
Fluoroscopes
C-arm

ABSTRACT

To simulate an early 20th century viral pneumonia radiotherapy treatment using modern fluoroscopy and evaluated it according to current dose guidelines. Monte Carlo was used to assess the dose distribution on an anthropomorphic phantom. Critical organs were: skin, breasts, esophagus, ribs, vertebrae, heart, thymus, and spinal cord. A 100 kV_p beam with 3 mm Al HVL, 25 × 25 cm² posterior-anterior (PA) field and 50 cm source-to-surface distance were simulated. Simulations had a resolution of 0.4 × 0.4 × 0.06 cm³ and a 6% uncertainty. Hundred percent dose was normalized to the skin surface and results were displayed in axial, coronal, and sagittal planes. Dose volume histograms were generated in MATLAB for further analysis. Prescription doses of 0.3, 0.5, and 1.0 Gy were applied to the 15% isodose for organ-dose comparison to current tolerances and potential risk of detriment. Ninety-five and ninety-seven percent of the right and left lung volumes, respectively, were well-covered by the 15% isodose line. For the 0.3, 0.5, and 1.0 Gy prescriptions, the maximum skin doses were 2.9, 4.8, and 9.6 Gy compared to a 2.0 Gy transient erythema dose threshold; left/right lung maximum doses were 1.44/1.46, 2.4/2.4, and 4.8/4.9 Gy compared to a 6.5 Gy pneumonitis and 30 Gy fibrosis thresholds; maximum heart doses were 0.5, 0.9, and 1.8 Gy compared to the 0.5 Gy ICRP-recommendation; maximum spinal cord doses were 1.4, 2.3, and 4.6 Gy compared to 7.0 Gy single fraction dose threshold. Maximum doses to other critical organs were below modern dose thresholds. A 100 kV_p PA field could deliver a 0.3 Gy or 0.5 Gy dose without risk of complications. However, a 1.0 Gy dose treatment could be problematic. Critical organ doses could be further reduced if more than one treatment field is used.

© 2020 American Association of Medical Dosimetrists. Published by Elsevier Inc. All rights reserved.

Introduction

In the early 20th century, viral and bacterial pneumonia patients were treated with radiotherapy to deliver lung doses of 0.3 to 1.0 Gy using 100 to 200 kV_p x-ray beams.¹⁻⁵ This was a

¹ Reprint requests to D. Roa, Department of Radiation Oncology, University of California, Irvine Health, Orange, CA 92868, USA.

E-mail address: droa@uci.edu (D. Roa).

one-time treatment and signs of recovery appeared as early as 3 to 5 hours after irradiation. Animal experiments of the time demonstrated that low radiation doses upregulated lymphocytosis and reduced inflammation.^{1,6,7} Today, modern studies support these conclusions.^{8,9} Unfortunately, radiotherapy treatments stopped in the 1940s with the advent of antibiotic- and steroid-therapies despite their high cure rate.¹

In light of the COVID-19 pandemic, there has been renewed interest in using low-dose radiotherapy as a treatment option for infected patients in critical condition, and when other treatments have failed to produce a cure.¹⁻³ Radiotherapy linear accelerators are the most effective technology for delivering such a treatment; however, the risk of infection to staff and cancer patients, as well as contamination of a radiation oncology clinic can be high despite rigorous procedure protocols. Modern fluoroscopes could be an alternative to deliver therapeutic radiation doses to the lungs using x-ray energies similar to those used historically. Fluoroscopes are more widely available worldwide than radiotherapy linear accelerators and could be used in intensive care units (ICUs) or emergency rooms (ERs) eliminating the need of patient transportation to a radiation oncology clinic.

It is worth exploring the dosimetry that a historical pneumonia treatment could have achieved via computer simulations using a modern kV x-ray beam from a fluoroscope on an anthropomorphic phantom. The simulations could justify an experimental verification with modern fluoroscopes and prove (or disprove) that they could be effective in delivering a low-dose radiotherapy treatment, since there are no modern data available and the field of dosimetry was not developed enough in the early 20th century to have historical data. Prescription dose¹⁻⁷ and technical information^{10-12, 15, 17, 18} can be extracted from published clinical and historical reports and used in the simulations.

In this study, prescription doses of 0.3, 0.5, and 1.0 Gy were used for isodose normalization while dose distributions and maximum doses to critical organs were evaluated according to modern dose tolerance guidelines. Results from this work and potential implementation using modern fluoroscopes are presented.

Materials and Methods

The Monte Carlo (MC) code PENELOPE with its mathematical anthropomorphic phantom was used for simulations.¹³ The phantom was an adult female anatomy that included most organs (Figs. 1a and 1b) with published density information for each of them. Each lung was 24 cm superior-inferior, 12 cm left-right, and 10 cm anterior-posterior. Organs-at-risk were: skin, breasts, ribs, esophagus, vertebrae, heart, thymus, and spinal cord. Skin volume was limited to the thoracic region only.

The SPEKTR 3.0¹⁴ code was used to generate a 100 kV_p x-ray beam spectrum from a tungsten target with an aluminum filter. Historically, a single- or 3-phase generator¹¹ would have produced significant ripple and a lower effective energy than a modern beam; however, 100 kV_p is at the bottom of the cited energy range, so the effective energy should still be appropriate for the historical context. A report of that time recommends the use of a 3-mm Al filter for x-ray radiotherapy of the lungs,¹⁵ which would result in a half-value layer (HVL) of approximately 3 mm Al, assuming an inherent tube filtration similar to modern tubes and tube ripple appropriate for a 3-phase generator.¹ Thus, a 3-mm Al HVL was selected for the simulated beam, which is a slightly softer spectrum than on modern units.¹⁶

The simulated treatment consisted of a 25 × 25 cm² posterior-anterior (PA) field at 50 cm source-to-surface distance (SSD) (Fig. 1c). The field covered both lungs and could have been defined with an x-ray system of that time (Fig. 1d) which was used for radiography, fluoroscopy, and radiotherapy procedures.^{10-12, 15, 17, 18}

The simulations had a spatial resolution of 0.4 × 0.4 × 0.06 cm³ and an uncertainty of 6% for 2 × 10⁹ histories. Cumulative dose volume histograms (DVHs) were generated in MATLAB (MathWorks, Natick, MA) and the MATLAB DVH code was validated using a known data set prior to the actual data analysis. DVHs were generated for the left/right lungs, skin, left/right breasts, esophagus, ribs, vertebrae, heart, thymus, and spinal cord.

The skin surface dose was normalized to 100% and considered the reference dose calibration location. For the absolute dose analysis, the 15% isodose line was

normalized to a 0.3, 0.5, and 1.0 Gy prescription dose, respectively, to obtain absolute dose information. These doses were selected based on the historical treatment doses reported.¹⁻⁵ Mean and maximum relative doses for each organ-at-risk were extracted from the DVHs, normalized to each prescription dose, and evaluated against the International Commission on Radiological Protection (ICRP) and other reports for organ dose tolerance assessment.¹³⁻²²

Results

Figure 2a shows the percent depth dose at the phantom's central sagittal plane. Peak doses at 0.5, 3.0, 5.5, and 19.5 cm depths corresponding to ribs or vertebrae regions resulted from photoelectric interactions. The most prominent peak was in the ribs at 0.5 cm depth with a 325% maximum point dose. The second-most prominent was in the vertebrae at 3 cm depth with 225% maximum dose. Conversely, soft tissue regions showed a smooth dose deposition reduction as a function of depth.

Figures 2b-2d show axial, coronal, and sagittal isodoses. The 15% isodose provided coverage to both lungs with 95% and 97% of the right and left lung volumes covered as shown in the DVH (Fig. 3a). The maximum relative doses to the lungs were 72% (right) and 73% (left).

Table 1 shows mean and maximum relative and absolute doses for the lungs, skin, breasts, esophagus, ribs, vertebrae, heart, thymus, and spinal cord, after applying a 0.3, 0.5, and 1.0 Gy prescription dose normalization to the 15% isodose. Table 1 also includes dose tolerances provided by ICRP and other reports for evaluation.

The maximum dose to the skin exceeded 2.0 Gy¹⁹⁻²¹ (the transient erythema dose threshold) by 44%, 240%, and 480% for the 0.3, 0.5, and 1.0 Gy prescriptions, respectively. The heart maximum dose exceeded 0.5 Gy (the threshold for potential cardiovascular and blood circulatory effects) by 5%, 76%, and 352% for the 0.3, 0.5, and 1.0 Gy prescriptions, respectively.^{19, 21, 22}

The heart mean dose also exceeded this threshold by 42% for the 1.0 Gy prescription, while it remained below the threshold for the 0.3 Gy and 0.5 Gy prescriptions.

Maximum doses to the lungs did not pose any risk for pneumonitis (6.5 Gy threshold for acute exposure)^{19, 17} or fibrosis (30.0 Gy threshold)²³ for any prescription dose. The lung mean doses suggested that a prescription dose normalization to the 20% instead of the 15% isodose could have been used which would have resulted in lower doses to critical organs. Mean and maximum doses to the breast were below the proposed 1.0 Gy dose threshold at which the risk for developing secondary cancers increases in women younger than 40 years.²⁴

Ribs maximum doses (prescription dose) were 78% (0.3 Gy), 64% (0.5 Gy), and 28% (1.0 Gy) below the 30.0 Gy single-fraction dose threshold. Furthermore, the dose to 1 cm³ of the ribs' volume, for all prescriptions, was below the 22.0 Gy single-fraction dose threshold.^{27, 28} The vertebrae maximum doses (prescription dose) were 67% (0.3 Gy) and 45% (0.5 Gy) below, but 11% (1.0 Gy) above the 12.4 Gy single-fraction dose threshold.^{27, 28} Ribs and vertebrae maximum doses for all prescriptions far exceeded the ICRP 118 recommended limit of 2.0 Gy dose per fraction but not the cumulative dose limit of 50.0 Gy.¹⁹ Mean and maximum doses to other critical organs for all prescription doses were well within modern dose tolerances.

Discussion

Calabrese *et al.*¹ were the first to suggest re-visiting the role of radiotherapy to treat pneumonia, and now, this suggestion has a newfound relevance in light of the COVID-19 pandemic. The early radiotherapy treatments used 100 to 200 kV_p x-rays to deliver a 0.3 to 1.0 Gy single fraction treatments. These x-ray energies are comparable to those produced with modern fluoroscopes. Although fluoroscopes are intended for imaging, it could be possible for them to be used for treatment purposes in these extraordinary times. If the image receptor was covered with lead to drive the exposure rate to its maximum, treatment times to deliver a 0.3 Gy prescription dose to patient of comparable size as the simulated phantom could be 15 to 20 minutes with a mobile fluoroscope and 2 to 3 minutes with an interventional fluoroscope operating in digital acquisition (cine) mode. Specific treatment times would have to be determined based on the exposure rate of the fluoroscope being used, with longer treatments potentially broken up to allow for periods of tube cooling, if this becomes a concern.

This investigative dosimetric analysis provides quantitative information on dose distributions and detriments to organs from such radiation treatments and suggests a potential treatment delivery with bedside c-arm fluoroscopes in an inpatient setting.

For a simple treatment setup consisting of a PA field, the 15% isodose provided effective coverage to the lungs with 95% and 97%

¹ Calculated using IPeM 78 Spectrum Processor Version 3.0. The Institute of Physics and Engineering in Medicine. 2015.

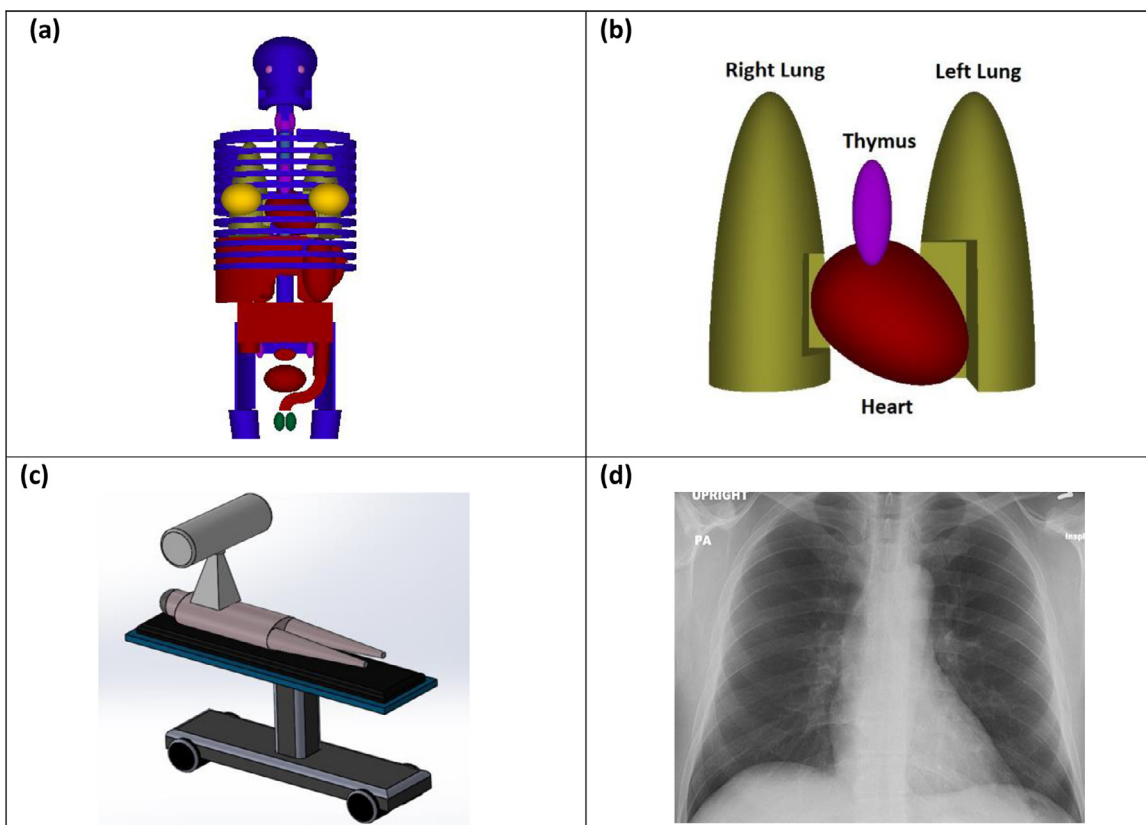


Fig. 1. (a) PENELOPE's mathematical anthropomorphic phantom of a female anatomy. (b) Thoracic anatomy inside the phantom. (c) Posterior-anterior treatment field used in the simulations. (d) Posterior-anterior tuberculosis chest x-ray during the first world war.¹⁷

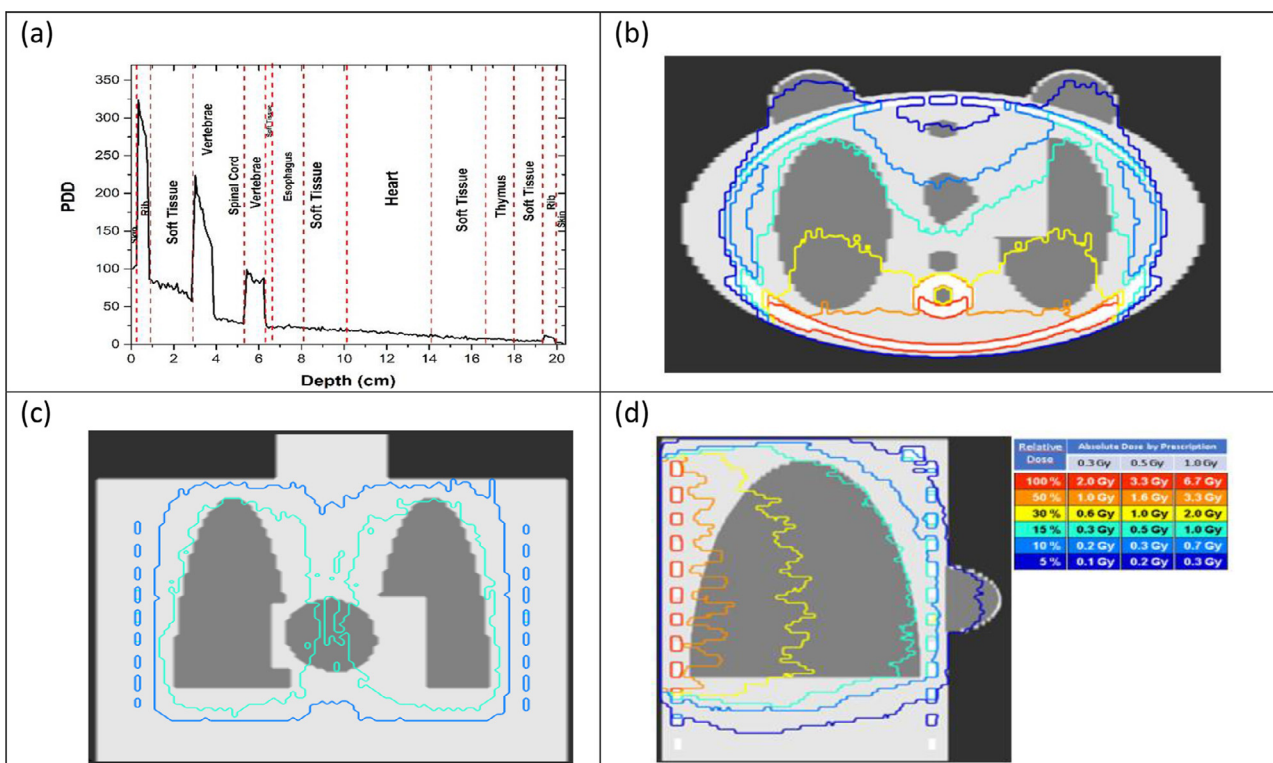


Fig. 2. Percent depth dose normalized to 100% at the skin surface (a) and dose (relative and absolute) distribution displayed in the axial (b), coronal (c), and sagittal (d) planes. The 15% isodose (cyan) distribution provided an effective dose coverage to both lungs. The 0.3, 0.5, and 1.0 Gy prescription dose, respectively, was normalized to the 15% isodose line for absolute dose analysis.

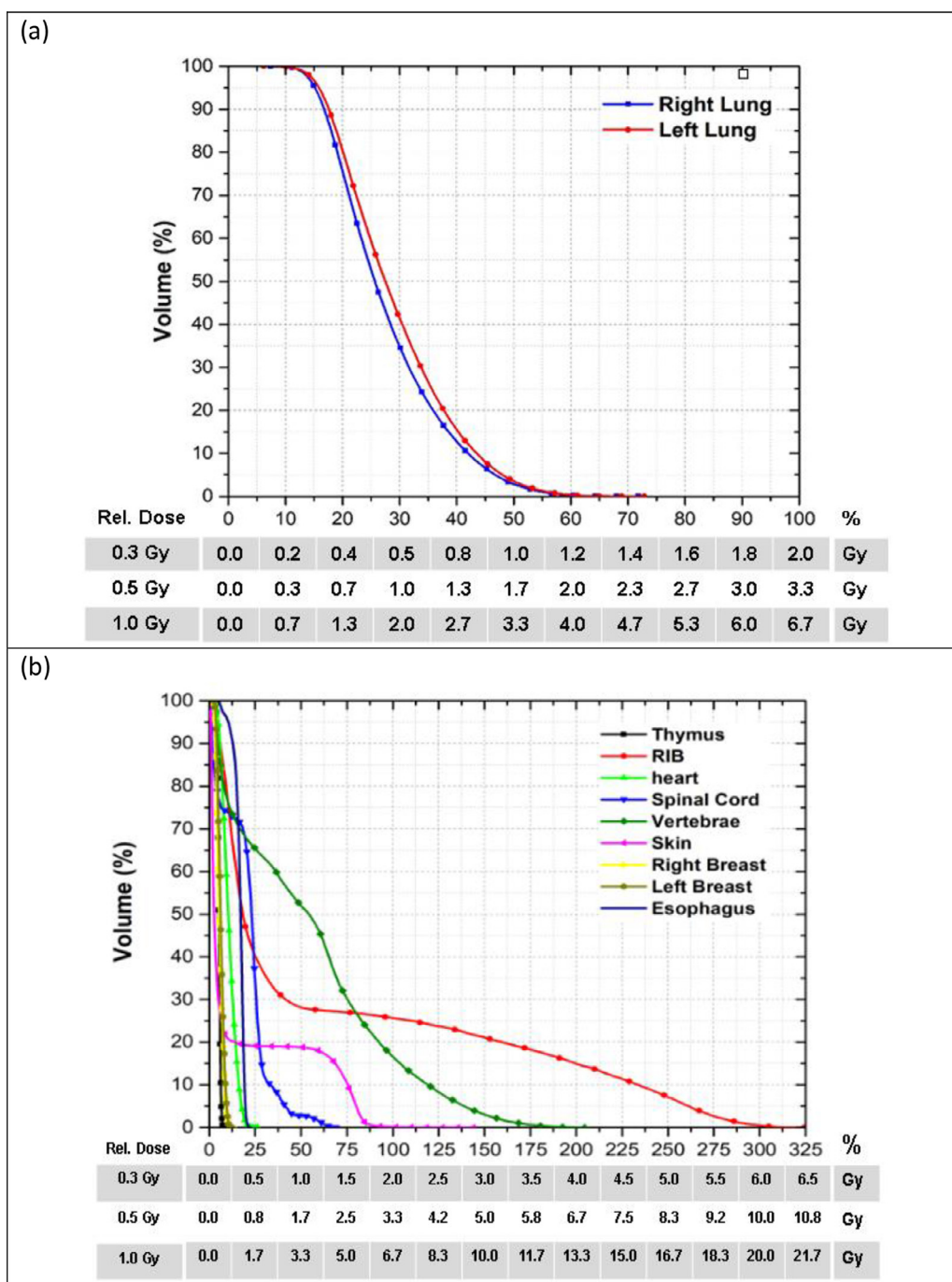


Fig. 3. Cumulative dose volume histograms that include relative and absolute doses for each the 0.3, 0.5, and 1.0 Gy prescription doses, for the right/left lungs (a) and organs at risk (b).

of the right and left lung volumes covered. After applying a 0.3, 0.5, or 1.0 Gy prescription dose to the 15% isodose, the maximum dose to the lungs did not exceed modern thresholds for pneumonitis or fibrosis.^{19,23} However, it could have exacerbated preradiation fibrosis caused by the pneumonia and/or affected patients with borderline interstitial fibrosis.

For the 0.3 and 0.5 Gy prescriptions, the resulting 2.0 to 5.0 Gy skin dose may produce signs of transient erythema within two weeks after exposure, recoverable epilation within 8 weeks, and no observable effects after 40 weeks.²⁰ For skin doses of 5.0 to 10.0 Gy, expected from a 1.0 Gy prescription, transient erythema

could manifest within 2 weeks, possible prolonged erythema and permanent epilation within 8 weeks, and at the upper end of the dose range, dermal atrophy and induration after 40 weeks.²⁰ It is likely that for the 0.3 and 0.5 Gy prescriptions, detrimental skin effects would not be permanent, but that may not be the case for a 1.0 Gy dose.

The 0.5 and 1.0 Gy prescriptions had maximum doses to the heart that significantly exceeded the 0.5 Gy dose threshold for possible cardiovascular and blood circulatory effects according to the ICRP 118 report.¹⁹ The ICRP 120 report²¹ supports the 0.5 Gy threshold statement; however, it adds that some uncertainty

Table 1

Mean and maximum relative and absolute doses are shown for prescription doses of 0.3, 0.5, and 1.0 Gy normalized to the 15% isodose line and compared to modern dose tolerance data.

Organ	Relative dose		0.3 Gy prescription		0.5 Gy prescription		1.0 Gy prescription		Modern dose tolerances
	Mean (%)	Max (%)	Mean (Gy)	Max (Gy)	Mean (Gy)	Max (Gy)	Mean (Gy)	Max (Gy)	
Right lung	27.6	71.8	0.55	1.44	0.92	2.40	1.84	4.79	6.5 Gy ¹⁹ (pneumonitis) 30.0 Gy ²³ (fibrosis)
Left lung	29.0	72.8	0.58	1.46	0.97	2.43	1.93	4.86	
Skin	16.3	144.0	0.33	2.88	0.54	4.80	1.09	9.60	2.0 Gy ²⁰ (transient erythema)
Right breast	5.6	12.6	0.11	0.25	0.19	0.42	0.37	0.84	1.0 Gy < For < age 40 2.5 fold risk ²⁴ For age 40 <.no excess risk ²⁴
Left breast	6.3	12.4	0.13	0.25	0.21	0.41	0.42	0.83	
Ribs	66.4	324.0	1.33	6.48	2.21	10.80	4.43	21.60	<30.0 Gy ^{27,28} single fraction 22.0 Gy for < 1 cc 12.4 to 14.0 Gy ^{27,28} single fraction
Vertebrae	54.8	204.5	1.10	4.09	1.83	6.82	3.65	13.64	0.5 Gy ^{19,21} 3.0 to 4.0 Gy ²²
Heart	10.6	26.3	0.21	0.53	0.35	0.88	0.71	1.76	0.71 Gy ²⁶
Thymus	5.3	8.4	0.11	0.17	0.18	0.28	0.35	0.56	7.0 Gy ^{27,28} single fraction
Spinal cord	20.3	69.1	0.41	1.38	0.68	2.30	1.35	4.60	40.0 to 45.0 Gy ²⁵ (acute esophagitis) < 34.0 Gy ²⁸ (mean dose)
Esophagus	16.4	22.4	0.33	0.45	0.55	0.75	1.09	1.50	

remains at this threshold. Other studies suggest that the risk of radiation-related heart disease from a low-dose radiotherapy can begin to manifest at 3.0 to 4.0 Gy.²² It is possible that a maximum heart dose of 0.9 Gy (0.5 Gy prescription) or 1.8 Gy (1.0 Gy prescription) could cause microvascular damage to the myocardium; however, the risk for heart-related complications would be low. Furthermore, peak skin doses from modern interventional cardiac procedures routinely exceed 2.0 to 3.0 Gy,²⁹ which implies that cardiac doses over 0.5 Gy are frequent and not an impediment to treatment. The 0.3 Gy prescription did not exceed this limit.

Maximum doses to the ribs and vertebrae for all prescriptions were below dose thresholds for a single fraction treatment.^{27,28} However, they far exceeded ($\geq 200\%$) the recommended ICRP 118 fractionated dose of 2.0 Gy.¹⁹ Although the risk of radionecrosis, rib fracture, and/or musculoskeletal atrophy would be low, no additional treatments without risk of complications would be possible with this setup. Additional treatment fields, such as anterior-posterior (AP) or laterals, could reduce maximum doses to these structures, but not below 2.0 Gy at the higher prescribed doses.

Published reports indicate that women under the age of 40 could have a 2.5-fold greater risk of secondary cancers if exposed to a dose greater than 1.0 Gy, compared to no risk for older women 10 years after irradiation.²⁴ In this work, mean doses to the breasts were below this level suggesting little-to-no detrimental effects. Maximum doses to the spinal cord, esophagus, and thymus were within modern dose tolerances and did not pose risk of future detriment.^{19,25-28}

This study indicates that a radiotherapy pneumonia treatment with a single PA field and a 0.3 or 0.5 Gy prescription dose to both lungs would have a low probability of radiation-induced detriment to critical organs. However, a 1.0 Gy dose treatment might be problematic. Treatment setups employing more fields could result in a more homogeneous dose distribution to the lungs, and lower dose to critical organs; this is an area of future work.

Treatment setups with 2 or more fields and hardened beams are possible with modern fluoroscopes. Fixed interventional c-arms could be ideal due to their large, highly filtered x-ray beams, higher x-ray tube heat capacities, and ease of positioning. Mobile c-arms could also be used for this purpose, albeit with longer treatment times but with the convenience of an in-situ treatment delivery. Modern mobile fluoroscopes do not have field sizes as

large as those simulated; however, therapy covering the entire lung field is possible with multiple beam angles.

A modified fluoroscopy unit with a larger field size might be possible with manufacturer support. While such a system may not be legally used for imaging in the United States, it could potentially be used as an investigational device under IRB approval. Perhaps another option could be the use of existing fluoroscopes on targeted treatments to affected areas identified on CT.³⁰

The prospect of rapid, inexpensive, and noninvasive therapy to reduce or prevent ventilator requirements could be paradigm-changing for centers with limited ventilator supplies. Clinical trials to evaluate the efficacy of low-dose radiation with linear accelerators for COVID-19 patients are underway in India, Iran, Italy, Spain, and the United States. However, there are no trials exploring the use of a fluoroscope-based delivery.

Low-dose treatments (0.3 to 0.5 Gy) via mobile c-arm fluoroscope in situ (e.g., at the patient bedside in intensive care units or emergency rooms) could prevent viral spread, contamination of radiotherapy clinics and other hospital spaces, and could be cost effective. The benefit-to-risk ratio is especially high for the elderly patients, who are more susceptible to complications from COVID-19 and less likely to develop radiation-induced cancers.³¹ Whereas the radiobiologic response remains to be explored further in COVID-19 pneumonia,³² the implementation of a safe, illness-reducing therapy delivered with fluoroscopy technology could be immediately implemented. Patients in low- to middle-income countries could have access to a viable life-saving treatment until a more definitive cure becomes available.

Conclusion

This study suggests that radiotherapy using a 100 kV_p x-ray source could be used to deliver a 0.3 or 0.5 Gy prescription dose to the lungs, with negligible risk of pneumonitis or fibrosis.

Maximum dose to the skin could cause transient erythema that resolves over time. A 1.0 Gy prescription dose, however, may result in more serious or long-term complications unless additional treatment fields are employed to reduce the maximum doses to critical organs.

Conflicts of Interest

The authors declare no conflicts of interest.

Acknowledgments

The authors would like to thank Professor Mauro Valente of the University of Cordoba, Argentina for his support with the Monte Carlo simulations.

No financial support was received for this project.

References

- Calabrese, E.J.; Dhawan, G. How radiotherapy was historically used to treat pneumonia: could it be useful today? *Yale J. Biol. Med.* **86**:555–70; 2013.
- Kirkby, C.; Mackenzie, M. Is low dose radiation therapy a potential treatment for COVID-19 pneumonia? *Radiother. Oncol.* 2020. doi:10.1016/j.radonc.2020.04.004.
- Dhawan, G.; Kapoor, R.; Dhawan, R.; et al. Low dose radiation therapy as a potential life-saving treatment for COVID-19-induced acute respiratory distress syndrome (ARDS). *Radiother. Oncol.* 2020. doi:10.1016/j.radonc.2020.05.002.
- Oppenheimer, A. Roentgen therapy for interstitial pneumonia. *J. Pediatr.* **23**(5):534–8; 1943.
- Desjardins, A.U. Radiotherapy for inflammatory conditions. *J. Am. Med. Assoc.* **96**:401–8; 1931.
- Fried, C. The roentgen treatment of experimental pneumonia in the guinea-pig. *Radiology* **37**:197–202; 1941.
- Glenn, J.C. Further studies on the influence of X-rays on the phagocytic indices of healthy rabbits. *J. Immunol.* **53**:95–100; 1946.
- Arenas, M.; Sabater, S.; Hernandez, V.; et al. Anti-inflammatory effects of low-dose radiotherapy. *Strahlenther. Onkol.* **188**:975–81; 2012.
- Lara, P.C.; Burgos, J.; Macias, D. Low dose lung radiotherapy for COVID-19 pneumonia. The rationale for a cost-effective anti-inflammatory treatment. *Clin. Transl. Radiat. Oncol.* **23**:27–9; 2020 444.
- Haus, A.G.; Cullinan, J.E. Screen film processing systems for medical radiography: a historical review. *Radiographics* **9**(6):1203–24; 1989.
- Krohmer, J.S. Radiography and fluoroscopy, 1920 to the present. *Radiographics.* **9**(6):1129–53; 1989.
- Mould, R.F. The early history of x-ray diagnosis with emphasis on the contributions of physics 1895–1915. *Phys. Med. Biol.* **40**:1741–87; 1995.
- Sempau, J.; Badal, A.; Brualla, L. A PENELOPE-based system for the automated Monte Carlo simulation of clinacs and voxelized geometries—application for far-from-axis fields. *Med. Phys.* **38**:5887–95; 2011.
- Punnoose, J.; Xu, J.; Sisniega, A.; et al. Technical note: SPEKTR 3.0—a computational tool for x-ray spectrum modeling and analysis. *Med. Phys.* **43**(8):4711–17; 2016.
- Knox, R. *Radiography and Radiotherapeutics Part 2: Radiotherapeutics*. New York: The Macmillan Company; 1919. p. 479.
- U.S. Code of Federal Regulations Title 21, Part 1020: Performance Standards for Ionizing Radiation Emitting Products. Rev. 4/1/2019. <https://www.accessdata.fda.gov/scripts/cdrh/cfdocs/cfcfr/CFRSearch.cfm?FR=1020.30>.
- Frederick Holmes M.D. Tuberculosis in the First World War. University of Kansas—School of Medicine. <http://www.kumc.edu/wwi/medicine/tuberculosis.html>.
- Williams, F.H.. *The Roentgen Rays in Medicine and Surgery as an Aid in Diagnosis and as a Therapeutic Agent*. New York: The Macmillan Company; 1903.
- ICRP ICRP statement on tissue reactions / early and late effects of radiation in normal tissues and organs – threshold doses for tissue reactions in a radiation protection context. ICRP Publication 118. *Ann. ICRP* **41**(1/2); 2012.
- Balter, S.; Miller, D.L. Patient skin reactions from interventional fluoroscopy procedures. *AJR* **202**:W335–42; 2014.
- ICRP Radiological protection in cardiology. ICRP Publication 120. *Ann. ICRP* **42**(1); 2013.
- Darby, S.C.; Cutter, D.J.; Boerma, M.; et al. Radiation-related heart disease: current knowledge and future prospects. *Int. J. Radiat. Oncol. Biol. Phys.* **76**(3):656–65; 2010.
- Rosen, I.I.; Fischer, T.A.; Antolak, J.A.; et al. Correlation between lung fibrosis and radiation therapy dose after concurrent radiation therapy and chemotherapy for limited small cell lung cancer. *Radiology* **221**:614–22; 2001.
- Stovall, M.; Smith, S.A.; Langholz, B.M.; et al. Dose to the contralateral breast from radiation therapy and risk of second primary breast cancer in the WECARE study. *Int. J. Radiat. Oncol. Biol. Phys.* **15**(4):1021–30; 2008.
- Werner-Wasik, M.; Yorke, E.; Deasy, J.; et al. Radiation dose-volume effects in the esophagus. *Int. J. Radiat. Oncol. Biol. Phys.* **76**(3):S86–93; 2010.
- Adams, M.J.; Dozier, A.; Shore, R.E.; et al. Breast cancer risk 55+ years after irradiation for an enlarged thymus and its implications for early childhood medical irradiation today. *Cancer Epidemiol. Biomarkers Prev.* **19**(1):48–58; 2010.
- Sahgal, A.; Chang, J.H.; Ma, L.; et al. Spinal cord dose tolerance to stereotactic body radiation therapy. *Int. J. Radiat. Oncol. Biol. Phys.*:1–13 2019. doi:10.1016/j.ijrobp.2019.09.038.
- Benedict, S.H.; Yenice, K.M.; Followill, D.; et al. Stereotactic body radiation therapy: the report of AAPM Task Group 101. *Med. Phys.* **37**(8):4078–101; 2010.
- Uniyal, S.C.; Chatuverdi, V.; Sharma, S.D.; et al. Patient dosimetry during interventional cardiac procedure in a dedicated catheterization laboratory. *Radiat. Prot. Dosimetry.* **175**(2):201–8; 2017.
- Simpson, S.; Kay, F.U.; Abbara, S.; et al. Radiological Society of North America expert consensus statement on reporting chest CT findings related to COVID-19. *J. Thorac. Imaging.* **2**(2); 2020. doi:10.1148/ryct.2020200152.
- Tubiana, M.; Diallo, I.; Chavaudra, J.; et al. A new method of assessing the dose-carcinogenic effect relationship in patients exposed to ionizing radiation. A concise presentation of preliminary data. *Health Phys.* **100**(3):296–9; 2011.
- Tharmalingam, H.; Díez, P.; Tsang, Y.; et al. Personal view: low-dose lung radiotherapy for COVID-19 pneumonia—the atypical science and the unknown collateral consequence. [published online ahead of print]. *Clin. Oncol.* 2020. doi:10.1016/j.clon.2020.06.002.